GEOLOGICA CARPATHICA, APRIL 2013, 64, 2, 133–140 doi: 10.2478/geoca-2013-0009

K/Ar mineral geochronology of the northern part of the Sithonia Plutonic Complex (Chalkidiki, Greece): implications for its thermal history and geodynamic interpretation

KYRIAKI PIPERA[1], ANTONIS KORONEOS[1], TRIANTAFYLLOS SOLDATOS[1], ZOLTÁN PÉCSKAY[2] and GEORGIOS CHRISTOFIDES[1]

[1]Department of Mineralogy, Petrology and Economic Geology, School of Geology, Aristotle University of Thessaloniki, 54124 Thessaloniki, Greece; heraia@geo.auth.gr; koroneos@geo.auth.gr; soldatos@geo.auth.gr; christof@geo.auth.gr
[2]Institute of Nuclear Research of the Hungarian Academy of Sciences, P.O. Box 51, Bém tér 18/c, H-4001 Debrecen, Hungary; pecskay@atomki.hu

(Manuscript received November 3, 2010; accepted in revised form October 16, 2012)

Abstract: New K/Ar mineral ages of thirty nine samples (biotite, muscovite, K-feldspar) from the two-mica granodiorite to granite and leucogranite of the northern part of the Sithonia Plutonic Complex (Chalkidiki, Greece) are given in the present study. These data along with existing Rb/Sr mica and U/Pb zircon ages are used to investigate the thermal history of the plutonic complex and shed light on the process that affected it, and caused discordant Rb/Sr and K/Ar mineral ages. The K/Ar mineral dating yielded ages ranging from 38 to 49 Ma for muscovites, 32 to 47 Ma for biotites and 37 to 43 Ma for K-feldspars, respectively. The comparison of the K/Ar, Rb/Sr and U/Pb mineral ages and the closure temperatures of the different isotopic systems for the different minerals indicate a rapid cooling rate for the Sithonia pluton. The latter supports the hypothesis that the pluton was formed in a post orogenic extensional regime. Moreover, the K/Ar mineral isochrones indicate that a reheating of the pluton took place before 37 Ma and partially rejuvenated the K/Ar and Rb/Sr isotopic system of the minerals.

Key words: Tertiary granitoids of Rhodope, Sithonia Plutonic Complex, K/Ar geochronology, thermal evolution.

Introduction

The origin, evolution and age of the Sithonia Plutonic Complex (SPC) intruding the Circum Rhodope Zone and Serbomacedonian Massif have been studied by many researchers (Soldatos & Sapountzis 1975; Sapountzis et al. 1976, 1979; De Wet & Miller 1986; Christofides et al. 1990, 1998, 2007; D'Amico et al. 1990; Perugini et al. 2003; Pipera et al. 2010; Melfos et al. 2012; Romanidis et al. 2012). The study of the Sithonia Eocene pluton is of great importance for the clarification of the geotectonic evolution of the Sidironero and Pangeon tectonic units of the Rhodope Massif since the Serbomacedonian Massif is considered equivalent to the Pangeon tectonic unit (Christofides et al. 2001). The age of the SPC was estimated from a whole rock Rb/Sr isochron on two-mica granodiorite samples which yielded 50.4±0.7 Ma (Christofides et al. 1990). This age is in accordance with the U/Pb zircon age of 51.32±0.89 Ma, obtained by Alagna et al. (2008). Christofides et al. (1990) attributed the low biotite Rb/Sr ages of some leucogranite samples to a rejuvenation of the Rb/Sr isotopic system during a tectonic event that took place at most 29 Myr ago. This rejuvenation was detected due to the disturbance of biotite ages. Further geochronological study of the pluton was necessary in order to examine this tectonic (thermal) event that took place and affected the pluton after the crystallization. The K/Ar dating, as a more "sensitive" dating method on temperature changes, was selected to work out the discordances of the previous resultant ages. Due to the lower closure temperatures of the minerals for the K/Ar isotopic system in respect to the Rb/Sr system, the former is more easily affected by any reheating and so it is more possible to detect any isotopic disturbance. The subject of the present study is the K/Ar mineral geochronology of the northern part of the Sithonia pluton. The systematic K/Ar study of the pluton in association with the previous geochronological studies sheds light on the pluton's thermal history after its emplacement and on its affinity with the geotectonic regime.

Analytical methods

The samples were crushed and the 150–250 μm grain size was collected. A vibrating table and a Franz Isodynamic Magnetic separator (model L-1) were used to separate muscovite and biotite. K-feldspar was extracted using the same magnetic separator and the heavy liquid tetrabromoethane ($Br_2CHCHBr_2$). The separation of the minerals was performed at the Department of Mineralogy, Petrology and Economic Geology, Aristotle University of Thessaloniki, Greece. Muscovite and biotite chemical analyses were performed on a JEOL scanning electron microscope at the Department of Mineralogy, Petrology and Economic Geology, Aristotle University of Thessaloniki, Greece. The operating conditions were: 20 kV and 20 nA, with a beam diameter <1 mm.

X-Ray Powder Diffraction analyses (XRPD) were performed on each mineral extract to calculate the proportion of

mineral and the purity of it. Powder XRPD analyses were obtained on a PHILIPS PW1820/00 X-ray diffractometer of the Department of Mineralogy, Petrology and Economic Geology, School of Geology, Aristotle University of Thessaloniki, carrying a PW1710 microprocessor. The operating conditions for all samples were 35 kV and 25 mA using Ni-filtered CuKζ radiation. The 2-theta scanning range was between 3° and 63° and the scanning speed was 1.2 °/min. Refinements were done with the PCAPD software and the identification of the samples was done with the JCPDS-ICDD 2003 database. The purity of biotite and muscovite was calculated over 98 % and of K-feldspar over 96 %.

The K/Ar dating was performed at the Institute of Nuclear Research of the Hungarian Academy of Science (ATOMKI), Debrecen, Hungary following the method described by Balogh (1985). An argon extraction line and a mass spectrometer, both designed and built in the ATOMKI, were used for the Ar measurement. The rock was degassed by high frequency induction heating and the usual getter materials (Ti sponge, CuO, zeolite and cold traps) were used for cleaning Ar. The ^{38}Ar spike was introduced in the system with a gas pipette before the beginning of the degassing. The cleaned Ar was directly introduced into the mass spectrometer. The mass spectrometer was a magnetic sector type of 150 mm radius and 90 °C deflection and it was operating in static regime. Recording and evaluation of Ar spectrum was controlled by suitable software. For the potassium content analysis 0.1 g of finely ground sample was digested in HF with addition of H_2SO_4 and $HClO_4$ and finally dissolved in 0.2 M HCl. Potassium was determined by flame photometry with a Na buffer and Li internal standard.

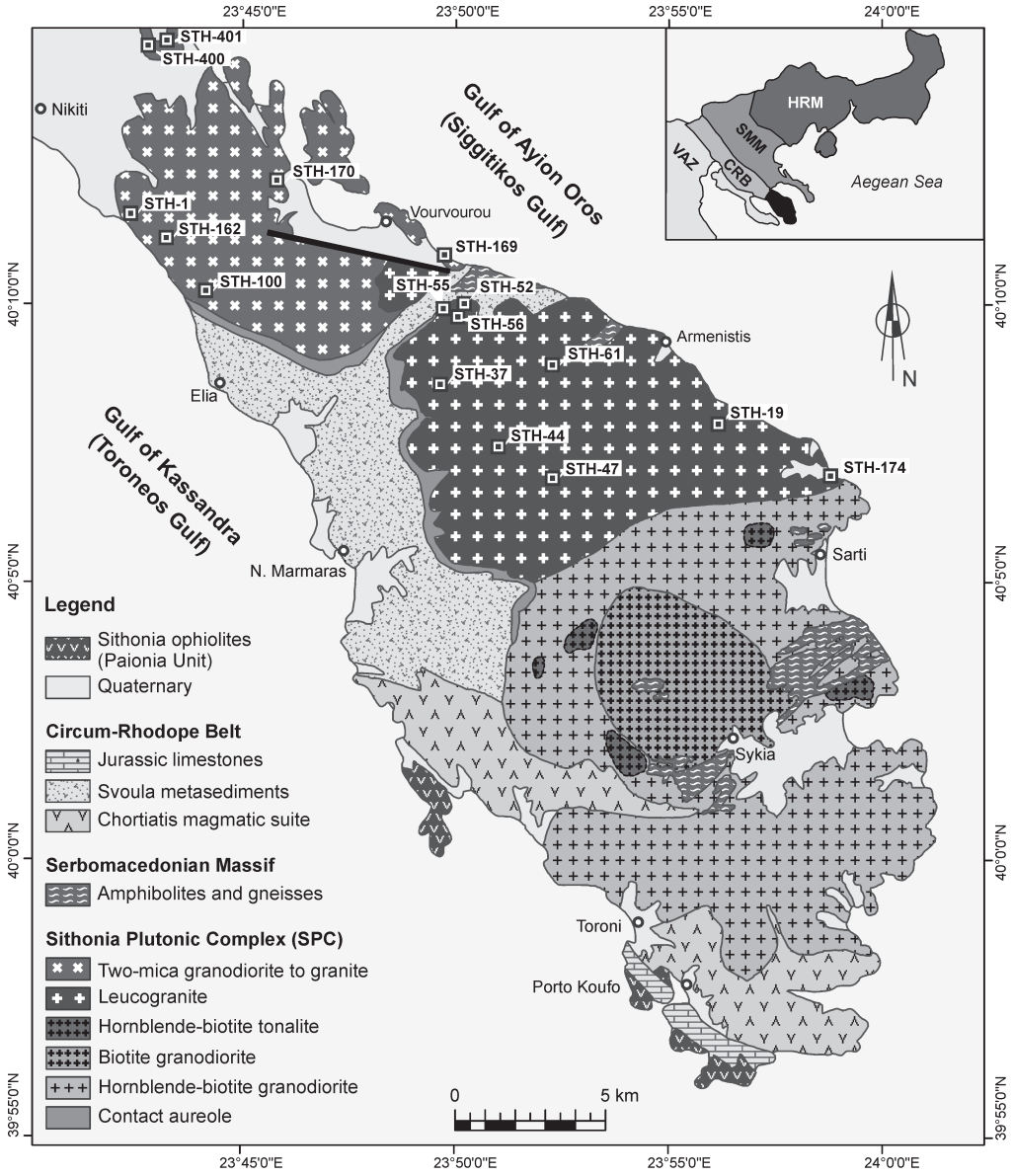

Fig. 1. Geological map of the Sithonia Plutonic Complex (SPC) and its country rocks including the sampling sites (modified map after Christofides et al. 2007). HRM – Hellenic Rhodope Massif, SMM – Serbomacedonian Massif, CRB – Circum-Rhodope Belt, VAZ – Vardar-Axios Zone.

Geological setting

The SPC occupies the greater part of the Sithonia Peninsula (about 350 km^2, Fig. 1) that constitutes the middle of the three peninsulas of Chalkidiki (Macedonia, N Greece). The bigger part of the Sithonia Peninsula belongs to the Circum Rhodope Belt while a minor occurrence of the Serbomacedonian Massif appears on the eastern part as well as a very limited occurrence of ophiolites of the Paionia Belt (Vergely 1984).

The intrusion of the SPC pluton caused contact aureole and affected the regional NW–SE strike of the schistosity and fold axes of the country rocks. The intrusion itself has been affected by younger tectonic activity that took place most probably in the Late Eocene–Oligocene and induced minor shear effects marked by mica orientation (Sakellariou 1989).

Over most of its outcrop, the SPC pluton reveals a planar fabric, which varies in intensity, but increases toward the margins. There is a magmatic foliation in the interior and a solid-state one in the marginal parts, where the fabric is planar-linear with the development of a WSW trending stretching lineation (Tranos et al. 1993).

The SPC consists of two-mica granite to granodiorite (TMG), leucogranite+porphyritic leucogranite (L+PLG) including many varieties of textural types, aplite and pegmatite (A), biotite granodiorite (BGd), hornblende-biotite granodiorite (HBGd), quartz-dioritic and tonalitic enclaves (MME) and hornblende-biotite granodioritic tonalite (Sapountzis et al. 1976, 1979; Christofides et al. 1990; D'Amico et al. 1990; Christofides et al. 2007). The LG intrudes the TMG to the north with sharp contacts and the HBGd to the south with transitional contacts. The BGd is younger than the HBGd and intrudes it clearly. Aplites and pegmatites occur all over the SPC intruding the pluton as well as the country rocks as the final products of the differentiation process. Tonalitic and monzonitic enclaves are found dispersed in all types except the TMG and PLG+LG.

Characteristics of the Sithonia Plutonic Complex

Geochemistry

The geochemistry of the SPC has been studied by Sapountzis et al. (1976, 1979), De Wet & Miller (1986), Christofides et al. (1990), D'Amico et al. (1990), Perugini et al. (2003), Christofides et al. (2007). The chemical composition of the SPC rocks ranging from tonalites to leucogranites corresponds to a chemical range of 62 % to 77 % SiO_2.

Petrography of the two-mica granodiorite to granite and leucogranites

The TMG body appears more or less homogeneous while the leucogranite displays textural variations so that several textural types can be distinguished. In the present paper the term PLG is applied to the more coarse-grained leucogranite often displaying porphyritic texture, while the term LG is applied to the more fine-grained leucogranite that occupies the eastern part of the pluton traversing the NE coast of the Sithonia Peninsula. Despite their modal and textural differences, both petrographic types are discussed together due to the similar mineralogy.

The essential mineral constituents are quartz, microcline, plagioclase, biotite and muscovite. Microcline is slightly perthitic and often displaying poikilitic texture enclosing plagioclase and mica. The plagioclase is usually subhedral. Discrete masses of leucogranite have microcline megacrysts which determines a porphyritic texture. The development of myrmekite among the grains is very frequent. Biotite and muscovite are euhedral to subhedral developed as individual macro-prismatic crystals sometimes oriented and elongated and often banded.

The accessory minerals are opaques (mostly ilmenite), apatite, zircon and locally, in the TMG only, epidote.

Mineral chemistry

Soldatos & Sapountzis (1975), Soldatos et al. (1976), D'Amico et al. (1990) and Christofides et al. (1998) studied the mineralogy of the SPC rocks. For the needs of the present study chemical analyses of muscovite and biotite of each sample analysed by the K/Ar method are presented.

Plagioclase appears in all rock types. It is usually zoned ranging from An_{34} to An_{10} in TMG, and An_{27} to An_8 in LG+PLG.

Microcline occurs as subhedral to anhedral interstitial crystals and also as megacrysts in some of the leucogranites. The composition ranges from O_{84} to O_{96} with the anorthite component not exceeding 1 %.

Biotite in the TMG and LG is associated with muscovite and is more Fe-rich compared with the other petrographic types. In Table 1 biotite analyses of the samples from the present study are presented.

Muscovite appears in large flakes and lath-shaped crystals, occurring singly, in clusters or intergrown with biotite and has characteristics favouring a primary origin. Large flakes resembling those of primary muscovite except for being slightly coloured and replacing feldspar are suggested to be of post-magmatic origin. Fine-grained secondary sericite also exists on plagioclase. On the basis of mode of occurrence and the TiO_2 content three types of muscovite are recognized (Table 2). The low-Ti (0.78–1.10 wt. %), moderate-Ti (1.18–1.58 wt. %) and the high-Ti (1.73–1.95 wt. %) muscovite.

Geochronological results

Dating was carried out on muscovite (Mu) and biotite (Bi) from all PLG samples, biotite, muscovite and K-feldspar (K-f) from all TMG samples except samples STH-400 and STH-401 where the muscovite concentration was very low, and on muscovite, biotite and K-feldspar from all LG samples. Table 3 summarizes the K/Ar mineral ages of all 39 analysed mineral samples.

The resultant ages of STH-170 and STH-400 biotite samples from TMG, STH-19 and STH-55 biotite samples from PLG and STH-169 and STH-174 biotite samples from LG have been subjected to Ar loss as indicated from their low $^{40}Ar_{rad}$ concentrations (<80 %) which causes younger result-

ant ages (Wörner et al. 2000; Panter et al. 2006). Regarding the results of the LG samples, it is obvious that they differ from those of the other two petrographic types. The ages are discordant in terms of mineral closure temperature principle Mu age>Bi age>K-f age. In detail, sample STH-169 K-f appears older or similar to biotite, taking into account the analytical error. Concerning Mu, Bi and K-f ages of sample STH-52 and Mu and K-f ages of sample STH-174 they are

Table 1: Representative analyses of TMG, PLG and LG biotites from the Sithonia Plutonic Complex. Each analysis represents the average of nine spots (three spots on each of three crystals).

	TMG						PLG							LG		
Sample	**1**	**100**	**162**	**170**	**400**	**401**	**19**	**37**	**44**	**47**	**55**	**56**	**61**	**52**	**169**	**174**
SiO_2	36.75	35.63	35.77	35.97	36.09	35.50	36.37	34.65	35.92	37.09	35.48	34.64	34.93	36.15	35.00	37.46
TiO_2	3.42	3.64	3.44	3.61	3.51	3.73	3.20	3.62	3.00	2.58	3.14	3.19	3.75	3.14	3.43	3.45
Al_2O_3	16.53	15.88	16.29	16.68	16.41	16.54	15.79	16.45	16.2	15.96	16.18	15.98	15.95	16.34	16.36	16.00
FeOt	21.88	23.44	23.28	22.95	22.87	23.83	22.84	25.23	24.45	22.69	24.77	24.82	24.89	23.18	24.33	22.41
MnO	0.26	0.36	0.22	0.11	0.27	0.82	0.76	0.65	0.45	1.00	0.30	0.42	0.32	0.29	0.67	0.86
MgO	7.99	8.03	7.47	7.74	7.84	6.61	7.94	6.31	6.88	7.76	7.35	7.65	7.01	7.88	6.81	7.08
CaO	0.07	0	0.10	0	0	0	0	0.23	0	0	0.09	0	0	0	0	0
Na_2O	0	0	0	0	0.11	0.11	0.12	0.11	0	0.10	0	0.24	0.10	0.18	0	0
K_2O	9.19	9.16	9.28	8.92	8.82	9.12	8.9	8.52	9.01	8.55	8.59	8.69	8.96	9.06	9.42	8.87
Total	96.07	96.16	95.84	95.98	95.92	96.26	95.92	95.78	95.91	95.73	95.88	95.62	95.91	96.21	96.02	96.13
Site allocations (22 O)																
Si	5.61	5.5	5.53	5.52	5.54	5.49	5.60	5.42	5.57	5.69	5.50	5.42	5.45	5.55	5.45	5.72
Al ^{IV}	2.39	2.50	2.47	2.48	2.46	2.51	2.40	2.58	2.43	2.31	2.50	2.58	2.55	2.45	2.55	2.28
Z	*8.00*	*8.00*	*8.00*	*8.00*	*8.00*	*8.00*	*8.00*	*8.00*	*8.00*	*8.00*	*8.00*	*8.00*	*8.00*	*8.00*	*8.00*	*8.00*
Al ^{VI}	0.58	0.39	0.49	0.53	0.51	0.50	0.47	0.45	0.53	0.58	0.46	0.37	0.38	0.53	0.46	0.60
Ti	0.39	0.42	0.40	0.42	0.41	0.43	0.37	0.43	0.35	0.3	0.37	0.37	0.44	0.37	0.40	0.40
Fe^{2+}	2.79	3.03	3.01	2.95	2.94	3.08	2.94	3.30	3.17	2.92	3.22	3.25	3.25	2.96	3.17	2.86
Mn	0.03	0.05	0.03	0.01	0.04	0.11	0.10	0.09	0.06	0.13	0.04	0.06	0.04	0.04	0.09	0.11
Mg	1.82	1.85	1.72	1.77	1.79	1.52	1.82	1.47	1.59	1.78	1.70	1.78	1.63	1.78	1.58	1.61
Y	*5.61*	*5.73*	*5.66*	*5.68*	*5.69*	*5.65*	*5.70*	*5.74*	*5.71*	*5.71*	*5.78*	*5.83*	*5.74*	*5.68*	*5.70*	*5.58*
Ca	0.01	0	0.02	0	0	0	0	0.04	0	0	0.01	0	0	0	0	0
Na	0	0	0	0	0.03	0.03	0.04	0.03	0	0.03	0	0.07	0.03	0.03	0	0
K	1.98	1.80	1.83	1.75	1.73	1.8	1.75	1.70	1.78	1.68	1.7	1.74	1.78	1.79	1.87	1.73
X	*2.00*	*1.80*	*1.85*	*1.75*	*1.76*	*1.83*	*1.79*	*1.77*	*1.78*	*1.71*	*1.71*	*1.81*	*1.81*	*1.82*	*1.87*	*1.73*

Table 2: Representative analyses of TMG, PLG and LG muscovites. Each analysis represents the average of nine spots (three spots on each of three crystals).

	TMG				PLG							LG				
Sample	**1**	**100**	**162**	**170**	**19**	**37**	**44**	**47**	**55**	**56**	**61**	**52***	**174***	**174**	**169***	**169**
SiO_2	46.70	45.90	46.37	45.50	46.56	46.5	45.83	46.11	45.96	45.37	46.07	45.85	45.84	46.19	46.13	45.82
TiO_2	1.44	1.58	1.42	1.45	1.26	1.21	1.30	1.28	1.18	1.73	1.36	0.78	1.10	1.57	1.05	1.95
Al_2O_3	31.49	31.21	29.86	31.7	30.18	32.22	31.25	31.08	32.1	31.63	32.33	32.87	30.55	29.76	31.93	32.23
FeOt	3.39	4.89	5.88	4.57	5.43	3.88	5.05	4.69	4.76	4.61	4.34	4.27	6.39	5.42	3.87	3.72
MgO	1.38	1.44	1.40	1.17	1.34	1.06	1.18	1.40	1.03	1.21	0.96	0.93	1.18	1.42	1.22	1.16
Na_2O	0.58	0.51	0.51	0.72	0.68	0.67	0.48	0.82	0.50	0.54	0.66	0.57	0.90	0.78	0.61	0.60
K_2O	10.60	10.59	10.74	10.64	10.88	10.90	10.92	10.86	10.79	10.72	10.15	10.72	10.07	10.72	10.72	10.37
Total	95.66	96.17	96.17	95.76	96.34	96.44	96.01	96.24	96.33	95.82	95.85	95.99	95.52	95.86	95.52	95.86
Site allocations (22 O)																
Si	6.30	6.21	6.31	6.18	6.32	6.25	6.23	6.26	6.21	6.16	6.20	6.20	6.25	5.27	6.25	6.16
Al ^{IV}	1.70	1.79	1.69	1.82	1.68	1.75	1.77	1.74	1.79	1.84	1.80	1.80	1.75	2.49	1.75	1.84
Z	*8.00*	*8.00*	*8.00*	*8.00*	*8.00*	*8.00*	*8.00*	*8.00*	*8.00*	*8.00*	*8.00*	*8.00*	*8.00*	*7.76*	*8.00*	*8.00*
Al ^{VI}	3.30	3.18	3.10	3.25	3.16	3.36	3.23	3.23	3.31	3.22	3.33	3.43	3.16	1.53	3.34	3.27
Ti	0.15	0.16	0.14	0.15	0.13	0.10	0.13	0.13	0.12	0.18	0.14	0.07	0.11	0.14	0.11	0.20
Fe^{2+}	0.38	0.55	0.67	0.52	0.62	0.44	0.57	0.53	0.54	0.52	0.49	0.48	0.73	0.52	0.44	0.42
Mg	0.28	0.29	0.28	0.24	0.27	0.21	0.24	0.28	0.17	0.24	0.19	0.19	0.24	0.24	0.25	0.23
Y	*4.10*	*4.19*	*4.20*	*4.15*	*4.17*	*4.11*	*4.18*	*4.17*	*4.15*	*4.17*	*4.15*	*4.17*	*4.24*	*3.55*	*4.13*	*0*
Na	0.08	0.08	0.02	0.13	0.03	0.09	0.02	0.04	0.09	0.07	0.14	0.05	0.12	0.10	0.08	0.16
K	1.82	1.83	1.87	1.84	1.89	1.87	1.89	1.88	1.86	1.86	1.74	1.85	1.75	1.55	1.85	1.78
X	*1.90*	*1.91*	*1.89*	*1.97*	*1.92*	*1.96*	*1.92*	*1.91*	*1.95*	*1.93*	*1.89*	*1.9*	*1.87*	*1.65*	*1.93*	*1.93*

*Low Ti muscovite

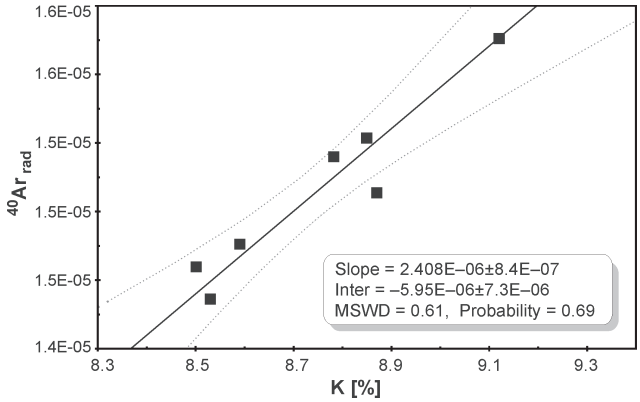

Fig. 5. $^{40}K/^{40}Ar$ isochron calculated for the PLG muscovites. The analytical error is 2 ω (68 % confidence level) and the MSWD = 0.61.

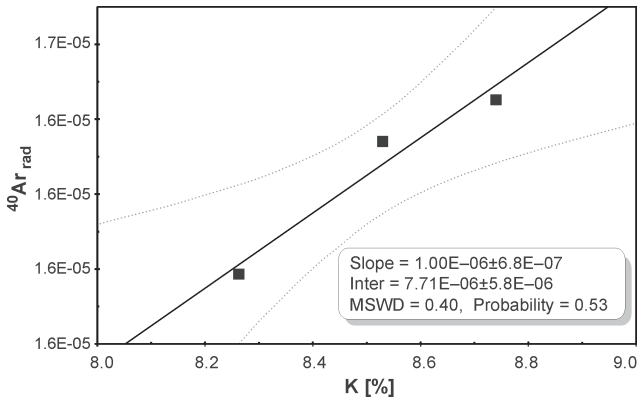

Fig. 6. $^{40}K/^{40}Ar$ isochron calculated for the TMG muscovites. The analytical error is 2 ω (68 % confidence level) and the MSWD = 0.40.

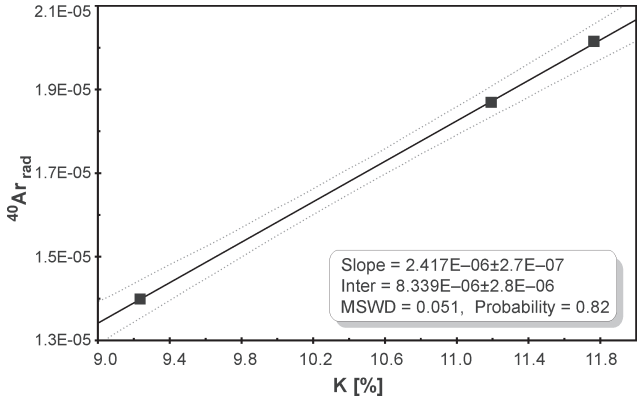

Fig. 7. $^{40}K/^{40}Ar$ isochron calculated for the TMG K-feldspars. The analytical error is 2 ω (68 % confidence level) and the MSWD = 0.051.

It must be stressed here that in the TMG isochron calculation, sample STH-170 was not included due to its younger age and its petrographic differences relative to the other TMG samples. The regression lines of TMG and PLG biotites do not constitute isochrons (MSWD = 2.8 and MSWD = 3.8 respectively) even though it seems that the biotites have not been subjected to Ar loss (Table 3). The regression lines of TMG and LG K-feldspars are isochrons with MSWD = 0.051 (Fig. 7) and 0.30 (Fig. 8) respectively.

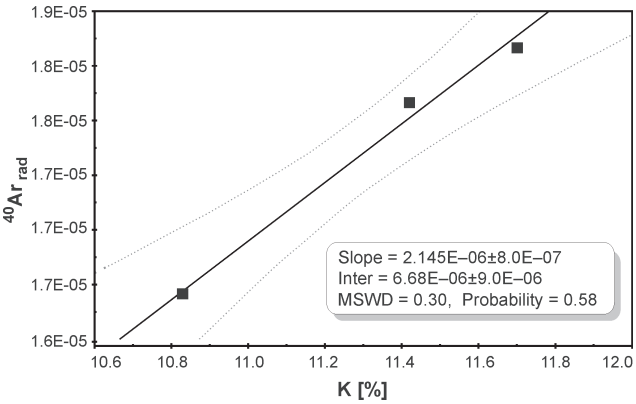

Fig. 8. $^{40}K/^{40}Ar$ isochron calculated for the LG K-feldspars. The analytical error is 2 ω (68 % confidence level) and the MSWD = 0.30.

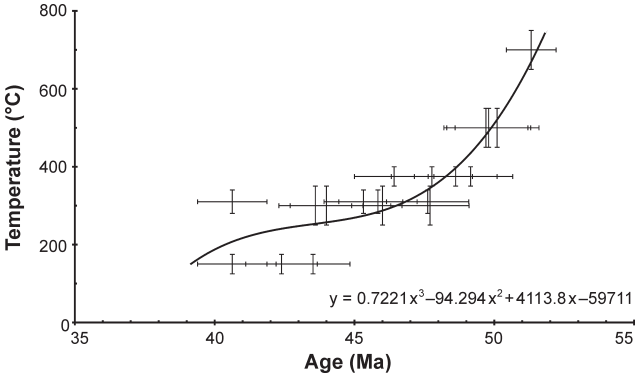

Fig. 9. Calculated trend line for the cooling rate of the TMG.

A cooling rate line for the TMG could be calculated based on the results of the present study, the Rb/Sr results of Christofides et al. (1990) and the zircon age of Alagna et al. (2008). In Fig. 9 the cooling trend line for the TMG samples is depicted. An average cooling rate of 51.8 ± 7.4 °C/Ma was calculated.

Discussion

Muscovite K/Ar results of all TMG and PLG samples gave undisturbed ages and isochron regression lines. PLG biotite and K-feldspar results do not form isochrons indicating a disturbance on the K/Ar isotopic system of these minerals. TMG biotite results do not form an isochron, but the TMG K-feldspars form a very good isochron.

The results of Christofides et al. (1990) were used in the present study for comparison between the two isotopic systems. Taking into account that the closure temperature of muscovite for the K/Ar isotopic system is lower (375 ± 25 °C; Jäger & Hunziker 1979; Harrison et al. 1985) than the closure temperature of the Rb/Sr system (500 ± 50 °C; Jäger &

Hunziker 1979), and the K/Ar system of our samples remained undisturbed, there is still more reason to expect the same for the Rb/Sr system. The Rb/Sr TMG muscovite results of Christofides et al. (1990) used for the calculation yielded an isochron MSWD=0.34 confirming the K/Ar isochron results. There are no Rb/Sr results for the PLG in order to carry out the same analysis.

Biotites of TMG and PLG show different behaviour than muscovites. Some samples from both types indicate Ar loss. For the rest of the samples regression lines were calculated but there was no K/Ar isochron formation either for the TMG or the PLG biotites. The Rb/Sr isotopic data for TMG were also used to calculate regression lines for biotites and, similarly, they do not form isochrons.

The behaviour of biotites could only be interpreted as the result of a thermal rejuvenation which reached the closure temperature of biotite for both K/Ar (310±30 °C; Jäger & Hunziker 1979; Harrison et al. 1985) and Rb/Sr systems (300±50 °C; Jäger & Hunziker 1979) and disturbed the K/Ar and Rb/Sr isotopic systems of biotites. Such rejuvenation should be attributed to a mild reheating event because the isotopic systems did not completely reset (Hayatsu & Carmichael 1970). A strong thermal event would have caused resetting of the isotopic systems and the regression lines would be isochrons indicating the age of the thermal event.

The K-feldspars of TMG and PLG indicate contrasting behaviour. TMG K-feldspars form isochrons but PLG K-feldspars do not. This probably means that the thermal reheating mentioned above was sufficient to rejuvenate the K-feldspars of TMG having a closure temperature of 150±25 °C (Lovera et al. 2002) but not those of PLG.

LG resultant ages are discordant and indicate different behaviour from the TMG and PLG samples. The muscovite regression line does not form an isochron and this is probably due to the two muscovite generations. The presence of the post-magmatic low Ti muscovite (Table 2) probably indicates another event that affected the LG. The muscovite ages in STH-52 and STH-174 are almost the same as the biotite and K-feldspar ages, respectively. The biotite ages are either not reliable (STH-174) or discordant in terms of isotopic closure (STH-52 and STH-174). The K-feldspar results seem to be unaffected forming isochrons and this is a very different behaviour compared to the other two minerals. The event affected the LG should be one of different nature than the reheating event affected the other two petrographic types. Field observations show that numerous and voluminous pegmatites intrude the LG. The frequency and intensity of this intrusion is not observable in the other petrographic types of SPC. Strachan et al. (1996), considers that the intrusion of numerous pegmatites could result in disturbance of the isotopic systems in terms not only of temperature but also of chemistry. Based on the Strachan et al. (1996) interpretation and on field observations, we suggest that LG muscovite and biotite isotopic systems were affected from the intrusion of the numerous pegmatites. The LG K-feldspar samples, probably affected from the thermal event previously discussed for TMG and PLG, rejuvenated from this pegmatitic event resulting in the homogenization of their isotopic system, and therefore gave a good isochron plot.

A recent fluid inclusions study (Melfos et al. 2012) of pegmatitic quartz from all over the SPC rocks gave remarkable results supporting the previous consideration. The fluid inclusions study, revealed the absence of primary fluid inclusions and the presence only of secondary or pseudo-secondary inclusions (probably due to a tectonic event). The homogenization temperatures vary between 270 and 310 °C with a peak at 290 °C that is very close to the closing temperature for K/Ar system in biotite. The only exception is the STH-5 sample (a pegmatite intruding LG) showing a second peak of homogenization temperatures at 230 °C. Thus, homogenization temperatures are in very good agreement with the results of the present study.

Regarding the age of the reheating, probably of tectonic origin as indicated from the fluid inclusions study, the younger resultant age of STH-400 K-feldspar (about 37 Ma) could be the upper limit for this thermal event because it is the younger reliable age measured. For the local event that disturbed the LG little can be said because of the unknown nature of this event. Probably it was imminent or younger than the reheating that affected also TMG and PLG.

The disturbance in mineral ages due to the mild thermal event did not result in important differences in ages, so the calculation of the cooling rate is more or less reliable if it is considered as a minimum due to the slightly younger K-feldspar ages.

The average cooling rate of the TMG as calculated above (average 51.8±7.4 °C/Ma) is very high. Fig. 9 shows that the cooling rate of TMG did not remain stable during the whole cooling history of the pluton. In general, the rapid cooling of plutons is attributed to extensional setting. According to Kilias et al. (2002) the extensional collapse in Rhodope Massif took place behind the orogenic arc in the back arc area during the Eocene/Oligocene. The geotectonic setting described by the latter workers interprets the rapid cooling of TMG calculated.

Conclusions

Biotites from the northern part of the Sithonia Plutonic Complex have been subjected to Rb/Sr and K/Ar isotopic disturbance as obtained from the discordances of their ages and the isochron plot results. Muscovite remained undisturbed resulting in good agreement with the existing dating of the pluton and the good isochron plots. K-feldspars of two-mica granodiorite (TMG) were rejuvenated from a reheating event which did not affect the K-feldspars of porphyritic leucogranite. A mild thermal event close to the closure temperature of biotite for the Rb/Sr and K/Ar closure temperature is considered to have affected the pluton isotopically. On the other hand, in a small area where the leucogranite (LG) outcrops, the voluminous pegmatitic intrusions seem to have affected locally the LG intrusion. This activity should be younger or imminent with the thermal event, which was probably of tectonic origin according to recent fluid inclusion studies. The age of the thermal event has a maximum of 37 Ma and the cooling rate that was calculated for the TMG is very high. The rapid cooling of the pluton is attributed to the extensional collapse of the Rhodope Massif during the Eocene/Oligocene when the SPC intruded.

Acknowledgments: The authors would deeply like to thank Prof. Eleftheriades G. for his valuable assistance on mineral separation, Lecturer Papadopoulou L. for her valuable assistance during the microprobe analyses and the PhD student Theodosoglou E. for her help in mineral separation. Critical reviews by Peter Marchev, Igor Petrík and one anonymous reviewer helped as improve the paper.

References

Alagna E.K., Petrelli M., Perugini D. & Poli G. 2008: Micro-analytical zircon and monazite U-Pb isotope dating by laser ablation-inductively coupled plasma-Quadrupole mass spectrometry. *Geost. and Geolan. Res*. 32, 1, 103–120.

Balogh K. 1985: K/Ar dating of Neogene volcanic activity in Hungary: experimental technique, experiences and methods of chronological studies. *MS ATOMKI Rep. D/1*, 277–288.

Christofides G., D'Amico C., Del Moro A., Eleftheriadis G. & Kyriakopoulos C. 1986: A Rb/Sr study on the granitoids of the Sithonia Peninsula (Northern Grece). *Terra Cognita* 6, 2, 142.

Christofides G., D'Amico C., Del Moro A., Eleftheriadis G. & Kyriakopoulos C. 1990: Rb/Sr geochronology and geochemical characters of the Sithonia plutonic complex (Greece). *Eur. J. Mineral*. 2, 1, 79–87.

Christofides G., Eleftheriadis G., Neiva M.A., Vlahou M. & Papadopoulou L. 1998: Major and trace element geochemistry of micas and amphiboles of the Sithonia pluton (Chalkidiki, N. Greece): constraints on its evolution. *Bull. Geol. Soc. Greece* XXXII/3, 231–240.

Christofides G., Koroneos A., Soldatos T., Eleftheriadis G. & Kilias A. 2001: Eocene magmatism (Sithonia and Elatia plutons) in the Internal Hellenides and implications for Eocene–Miocene geological evolution of the Rhodope Massif (Northern Greece). *Acta Vulcanol.* 13, 1–2, 73–89.

Christofides G., Perugini D., Koroneos A., Soldatos T., Poli G., Eleftheriadis G., Del Moro A. & Neiva A.M. 2007: Interplay between geochemistry and magma dynamics during magma interaction: An example from the Sithonia Plutonic Complex (NE Greece). *Lithos* 95, 243–266.

D'Amico C., Christofides G., Eleftheriades G., Bargossi G.M., Campana R. & Soldatos T. 1990: The Sithonia Plutonic Complex (Chalkidiki, Greece). *Mineral. Petrog. Acta* 33, 143–177.

De Wet A.P. & Miller J.A. 1986: ^{40}Ar–^{39}Ar data from some of the granitoids of the Chalkidiki peninsula, Northern Greece. ICOG VI. *Terra Cognita*, 6, 2, suppl. abs.

Harrison T.M., Duncan I. & McDougall I. 1985: Diffusion of ^{40Ar} in biotite: temperature, pressure and compositional effects. *Geochim. Cosmochim. Acta* 49, 2461–2468.

Hayatsu A. & Carmichael M.C. 1970: K/Ar isochron method and initial argon ratios. *Earth and Planet. Sci. Lett*. 8, 71–76.

Jäger E. & Hunziker K. 1979: Introduction to geochronology. *Springer Verlag*, New York, 1–329.

Kenneth L.R. 2008: A geochronological toolkit for Microsoft Office Excel. *Berkley Geochronology Center, Spec. Publ*., 1–4.

Kilias A.A., Tranos D.M., Orozco M., Alonso-Chaves M.F. & Soto I.J. 2002: Extensional collapse of the Hellenides: A review. *Rev. Soc. Geol*., *España* 15, 3–4, 129–139.

Kockel F., Mollat H. & Walther H. 1977: Erläuterungen zur geologischen Karte der Chalkidiki und angrezender Gebiete 1:100,000. *Bundesanst. Geowiss. und Rohstoffe*, Hannover, 1–119.

Lovera O.M., Grove M. & Harrison M.T. 2002: Systematic analysis of K-feldspar $^{40}Ar/^{39}Ar$ step heating. Results II. Relevance of laboratory argon diffusion properties to nature. *Geochim. Cosmochim. Acta* 66, 7, 1237–1255.

Melfos V., Stamatiadis A., Pipera K. & Christofides G. 2012: Fluid inclusion study in the pegmatites of the Sithonia Plutonic Complex, Chalkidiki, N. Greece. *Scientific Annals, Geology Department, Aristotle University of Thessaloniki, Spec. Issue* 101, 55–61.

Panter K.S., Blusztajn J., Hart S.R., Kyle P.R., Esser R. & McIntosh W.C. 2006: The origin of HIMU in the SW Pacific: Evidence from intraplate volcanism in southern New Zealand and subantarctic islands. *J. Petrology* 47, 1673–1704.

Perugini D., Poli G., Christofides G. & Eleftheriadis G. 2003: Magma mixing in the Sithonia Complex, Greece: evidence from mafic microgranular enclaves. *Miner. Petrology* 78, 173–200.

Pipera K., Koroneos A., Soldatos T., Pécskay Z. & Christofides G. 2010: K/Ar mineral geochronology of the northern part of the Sithonia Plutonic Complex (Chalkidiki, Greece) and implications for its thermal history. *XIX Congress of the Carpathian-Balkan Geological Association, Abstracts Vol*., 311–312.

Romanidis G., Christofides G., Koroneos A., Pécskay Z. & Soldatos T. 2012: K/Ar dating and thermochronology of the South Sithonia Plutonic Complex (Chalkidiki, Greece). *Scientific Annals, Geology Department, Aristotle University of Thessaloniki, Spec. Issue* 101, 111–118.

Sakellariou D. 1989: Geologie des Serbomazedonischen Massivs in der Nordoestlichen Chalkidiki, N. Griechenland – Deformation und Metamorphose. *Diss. Mainz. Univ., Geol. Monographs No. 2, Dept. of Geology, Univ. Athens*, 1–177.

Sapountzis E., Soldatos K., Eleftheriades G. & Christofides G. 1976: Contribution to the study of the Sithonia Plutonic Complex (N. Greece). II. Petrography–Petrogenesis. *Ann. Geol. Pays Hellén*. 28, 99–134.

Sapountzis S.E., Soldatos K., Eleftheriades G. & Christofides G. 1979: Contribution to the study of the Sithonia Plutonite. *Ann. Geol. Pays Hellén*. 30, 421–430 (in Greek).

Soldatos K. & Sapountzis S.E. 1975: Myrmekite of the Sithonia granodiorite. *Sci. Ann., Fac. Phys. & Mathem., Univ. Thessaloniki* 15, 391–407.

Soldatos K., Sapountzis S.E., Christofides G. & Eleftheriadis G. 1976: Contribution to the study of the Sithonia plutonic complex (N. Greece). I. Mineralogy. *Ann. Geol. Pays Hellén*. 28, 62–98.

Stamatiadis A. 2010: Fluid inclusions study in pegmatites from Sithonia Plutonic Complex Chalkidiki, Greece. *Diploma Thesis submitted at the Aristotle University of Thessaloniki*, 1–80.

Strachan A.R., Nance D.R., Dallmeyer D.R., D'Lemos S.R., Murphy B.J. & Watt R.G. 1996: Late Precambrian tectonothermal evolution of the Malverns Complex. *J. Geol. Soc., London* 153, 589–600.

Tranos M.D., Kilias A.A. & Mountrakis D.M. 1999: Emplacement and deformation of the Sithonia Granitoid Pluton (Macedonia, Hellas). Proc. 6th Cong., Geol. Soc. Greece, Athens 1993. *Bull. Geol. Soc*., Greece 2, 1, 195–210.

Vergely P. 1984: Tectonique des ophiolites dans le Hellenides internes. Consequences sur l'evolution des regions Tethysiennes occidentales. *These Doct. d'Etat, Paris/Sud*, 1–650.

Wörner G., Hammerschmidt K., Henjes-Kunst F., Lezaun J. & Wilke H. 2000: Geochronology (Ar-Ar, K/Ar and He-exposure ages) of Cenozoic magmatic rocks from northern Chile (18–22 °S): Implications for magmatism and tectonic evolution of the central Andes. *Rev. Geol*., *Chile* 27, 2, 205–240.